www.nature.com/scientificdata

scientific data

OPEN

DATA DESCRIPTOR

TSFabrics: A Time-Series Fabric Dataset for Real-Time Defect Detection on Circular Knitting Machines

Yan-Qin Ni[1], Pei-Kai Huang[2,3], Wei-Jen Wang[1], Deron Liang[1] & Chia-Yu Lin[1]✉

Existing fabric datasets consist of isolated and non-time-series images, failing to reflect the complexities and variations present in real-world industrial environments. To support fabric defect detection in real-world industrial environments, we present a high-quality Time-Series fabric dataset (TSfabrics). By capturing time-series fabric images, TSfabrics reflects the continuous and complex nature of actual fabric manufacturing on circular knitting machines. TSfabrics encompasses 22 continuous fabric production scenarios and consists of 93196 grayscale fabric images collected under diverse production conditions, including different illuminations, production speeds, and fabric types. In addition, TSfabrics contains defect-free and defective samples, with pixel-level annotations that differentiate true defects from production-related "cutlines" found in defect-free fabric images. Meanwhile, TSfabrics covers a wide range of fabric defect types. To sum up, TSfabrics offers a valuable resource for advancing practical fabric defect detection methods and bridging the gap between academic research and industrial application. We believe that TSfabrics enables the development and evaluation of defect detection models that are better suited for deployment on continuous production lines.

Background & Summary

Defect detection plays a vital role in industrial inspection[1–4], enabling the early identification of anomalies to ensure product quality, enhance production efficiency, and reduce manufacturing costs. Among various industrial applications, fabric defect detection has emerged as a critical task owing to the continuous and high-speed nature of textile production, where timely and accurate defect identification is essential for maintaining quality and minimizing losses. Fabric defect detection[5–7] aims to detect defects in newly manufactured fabrics, allowing timely alerts for operators to adjust knitting machines to enhance yield and reduce unnecessary production costs during the fabric manufacturing process. However, collecting abnormal data in industrial production is costly, leading to the scarcity of abnormal data. To alleviate the scarcity of abnormal data, many existing fabric defect detection methods[8–10] often adopted one-class classification techniques[11–14] to detect unseen types of anomalies during inference. Therefore, a high-quality fabric dataset that includes sufficient abnormal data is crucial[6,15] for advancing fabric defect detection. In particular, the inclusion of sufficient abnormal data in the dataset enables the training of detection models capable of more accurate and reliable defect identification, ultimately improving manufacturing efficiency.

There are several potential cost-related concerns associated with the collection of a high-quality fabric dataset. First, abnormal (defective) fabric images are difficult to obtain. In the fabric manufacturing process, owing to the typically high yield rate, collecting normal (defect-free) fabric images is relatively straightforward. In contrast, obtaining abnormal (defective) fabric images is significantly more challenging, as such samples often indicate production losses in real-world manufacturing environments. Second, annotating the ground truth is highly costly, as it requires extensive manual effort to accurately label defect locations in abnormal samples or production-marked areas in normal samples at the pixel level. Many existing studies[16–18] have made significant

[1]Department of Computer Science and Information Engineering, National Central University, Taoyuan City, Taiwan. [2]College of Computer and Cyber Security, Fujian Normal University, Fuzhou City, China. [3]Department of Computer Science, National Tsing Hua University, Hsinchu City, Taiwan. ✉e-mail: sallylin0121@ncu.edu.tw

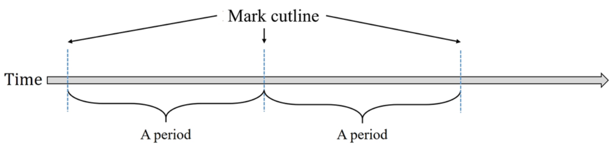

Fig. 1 Illustration of the production period in fabric manufacturing.

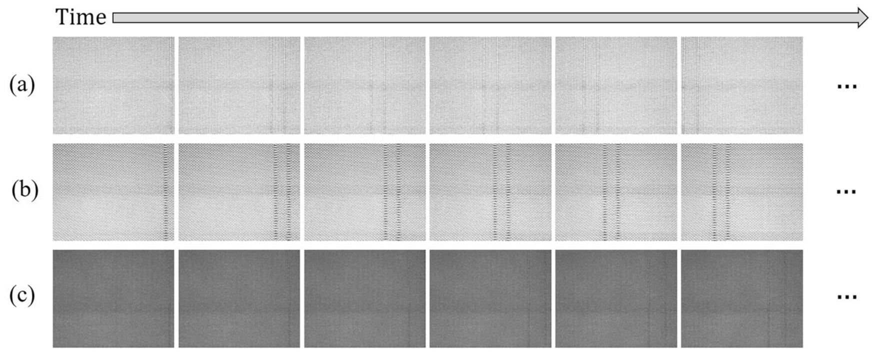

Fig. 2 Examples of defect-free time-series fabric images with "cutlines" collected from circular knitting machine production under different production speeds: (**a**) high speed, (**b**) regular speed, and (**c**) low speed.

efforts to collect fabric data. For example, the authors in[18] collected a fabric dataset named **YDFID-2**, which comprises yarn-dyed fabric defect samples obtained from an industrial enterprise, featuring 276 manually annotated defects. In addition, Zhang *et al.*[16] collected a fabric dataset named **ZJU-Leaper**, which comprises 98,777 fabric images across 19 distinct fabric categories, each with detailed annotations. These existing fabric datasets, built under idealized production conditions and consisting of individual and non-time-series fabric images, are valuable resources. **In real manufacturing, circular knitting machines produce fabrics in a continuous and uninterrupted manner**. However, these fabric datasets consist of individual and non-time-series images and lack continuous fabric image sequences that accurately reflect continuous knitting production scenarios. Hence, it remains uncertain whether fabric defect detection models trained on individual, non-time-series datasets can effectively detect defects when deployed on real production lines. Due to limitations in existing fabric datasets, which fail to reflect practical production conditions, the models trained on them often lack applicability in large-scale, continuous-knitting environments. There is a pressing need for time-series fabric datasets that capture the continuous nature of fabric production, enabling defect detection models to better meet the practical demands of real-world industrial manufacturing.

Fabric production using **circular knitting machines** is inherently continuous and sequential, with fabric produced in a steady, uninterrupted flow. As shown in Fig. 1, during continuous fabric production, circular knitting machines mark the fabric with a "cutline" after completing each full production cycle to facilitate subsequent manufacturing processes and cutting. This continuous process causes fabric images captured by a fixed-rate camera to form sequential frames instead of isolated and independent snapshots. Therefore, these marked cutlines should not be considered as defects. As existing non-time-series fabric datasets treat any texture variation within individual fabric images as a defect, fabric defect detection models trained solely on such individual images may mistakenly classify defect-free fabric images with cutlines (as shown in Fig. 2) as defective.

Unlike single static fabric images, continuous time-series fabric data capture both spatial and temporal information to reflect texture consistency and dynamic changes in the fabric over time. The availability of continuous fabric image sequences provides a critical advantage for fabric defect detection in real-world fabric manufacturing scenarios. First, time-series fabric images better reflect the continuous and complex nature of actual fabric manufacturing, as opposed to the idealized production conditions represented by individual fabric images. Next, time-series data allow fabric defect detection models to learn and exploit the inherent consistency and regularity of normal fabric patterns across adjacent frames, enabling the more effective identification of subtle or transient defects, such as weaving skips, yarn pulls, or minor color variations, that disrupt this temporal consistency. Therefore, continuous time-series fabric image data not only reflect real-world scenarios in industrial fabric production, but also significantly enhance the robustness and accuracy of defect detection systems compared with isolated fabric images. However, time-series fabric datasets remain unexplored in the field of fabric defect detection.

In this paper, to address the limitations of existing fabric datasets and better support real-world industrial fabric manufacturing, we introduce a high-quality **T**ime-**S**eries dataset, named **TSfabrics**, for fabric defect detection on circular knitting machines. First, we introduce the equipment required for collecting time-series fabric images. Figure 3 shows a circular knitting machine used in the production process along with the corresponding data collection equipment. Because the fabric output speed of a circular knitting machine varies depending on the type of knitted fabric during actual continuous production, the camera (Fig. 3(b)), operating

(a) (b) (c)

Fig. 3 Illustration of fabric image collection equipment, including (**a**) circular knitting machine, (**b**) camera sensor (marked in red box in (**a**)), and (**c**) storage computer (marked in black box in (**a**)).

at a fixed capture rate, can capture time-series fabric images that exhibit varying spatial intervals and motion patterns across different fabric types. The captured time-series fabric images were stored in the corresponding storage computers (Fig. 3(c)). Next, we introduce the characteristics of the proposed dataset (**TSfabrics**). **TSfabrics** not only accurately reflects real-world continuous knitting production scenarios through previously unexplored time-series fabric images, but also includes a diverse range of defect types, each accompanied by detailed pixel-level annotations. In particular, (**TSfabrics**) authentically captures **time-series** fabric images under diverse real-world production conditions, including (1) varying lighting environments, (2) different production speeds, and (3) multiple fabric types. In addition, **TSfabrics** encompasses a diverse range of fabric defect types, including (**a**) Dropped stitch, (**b**) hole, (**c**) missed stitch, (**d**) fiber lint, (**e**) oil stain, (**f**) distortion, and (**g**) color deviation. Furthermore, based on these diverse real-world production conditions, we design experiments to closely simulate real-world scenarios to evaluate the proposed **TSfabrics**. Our contributions are summarized as follows:

- We introduce a new **time-series** fabric dataset, named **TSfabrics**. To the best of our knowledge, this is the first fabric dataset that closely simulates real-world **continuous** fabric industrial manufacturing scenarios for fabric defect detection.
- **TSfabrics** is collected under diverse real-world production conditions—including varying lighting environments, different production speeds, and multiple fabric types—while also encompassing a wide range of fabric defect types.
- **TSfabrics** includes both defect-free and defective samples, each accompanied by detailed pixel-level annotations.
- Based on real factory production conditions, we design experiments that closely simulate real-world scenarios to evaluate the collected dataset.

Methodology

In this section, we introduce the proposed time-series fabric dataset (**TSfabrics**), which was collected from circular knitting machines. First, we present the equipment required for dataset acquisition. Next, we detail the pipeline for dataset collection.

Equipments of Data Collection. Figure 3 shows the essential equipment used for collecting time-series fabric images, including (a) a circular knitting machine, (b) a camera sensor, and (c) a storage computer. In particular, the camera model used was WP-UT050M, which lacks a photosensitive sensor, making the captured images sensitive to lighting conditions. In addition, the computer used for data collection is equipped with an Intel Core i7-8700 CPU, 64GB Kingston HyperX FURY DDR4-3200 RAM (16GB $\times$ 4), an MSI GeForce RTX 2080 Ti GAMING X TRIO GPU, and runs Windows 10 Professional 64-bit.

We employed an industrial camera (UI-5240CP, IDS Imaging Development Systems GmbH) for image acquisition. The camera is fitted with an 8 mm C-mount lens with a manual focus ring, enabling precise control of the imaging plane during high-speed fabric movement.

Image Acquisition. All images in TSfabrics are captured in grayscale. The sensor captures images at a native resolution of 1280 $\times$ 1024 pixels with a fixed frame rate of 30 fps. As a result, the dataset naturally includes sequential frames with partial spatial overlap. This temporal sequence reflects the continuous monitoring process in industrial knitting. All adjacent frames are captured in an uninterrupted time series and retained to preserve the realistic temporal characteristics of the production line, with no artificially duplicated frames. In addition, all fabric defects in the dataset are real defects occurring during production, rather than synthesized data.

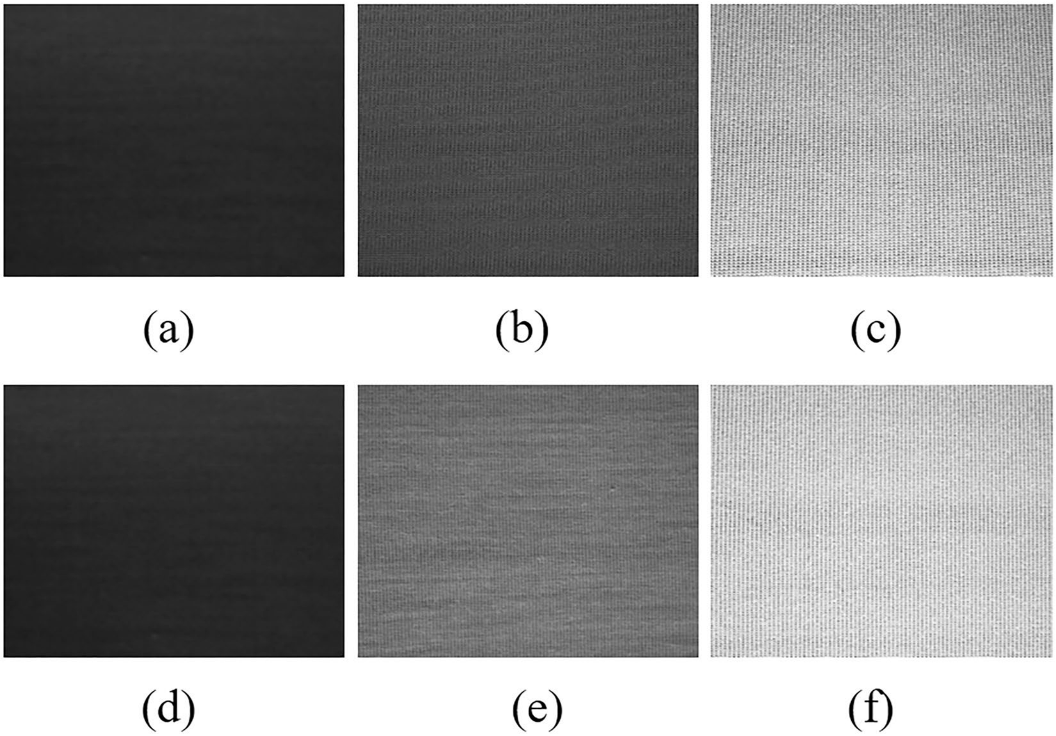

Fig. 4 Examples of defect-free fabric images (the same type of fabric with the same texture) under different illumination conditions: (**a**) and (**d**) dark illumination, (**b**) and (**e**) normal illumination, and (**c**) and (**f**) bright illumination.

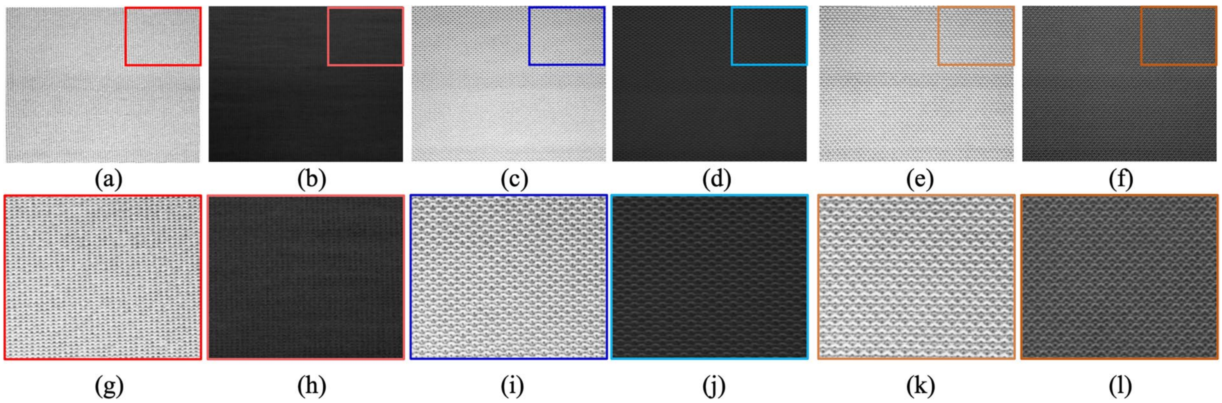

Fig. 5 Examples of different fabric textures under varying illumination conditions: (**a**), (**b**), (**g**) and (**h**) belong to Double Piqué (Plain Knit), (**c**), (**d**), (**i**) and (**j**) belong to Double Piqué (Four-Corner PK), and (**e**), (**f**), (**k**) and (**l**) belong to Double Piqué (Six-Corner PK).

Image Pre-processing. In **TSfabrics**, each fabric image is initially captured at a resolution of 1280 $\times$ 1024 pixels using a grayscale industrial camera. Due to the camera mount and the illumination geometry around the knitting zone, the four corners of the raw images exhibit slight shadowing and reduced brightness. To remove these boundary artifacts while preserving the central region where the fabric texture is clearly visible, we apply a center crop of 800 $\times$ 640 pixels to each image. This cropped area retains the uniformly illuminated region and excludes non-informative peripheral content. Figure 6 shows the cropping process. Since 800 $\times$ 640 pixels correspond to a physical size of 16 cm $\times$ 13 cm, the dataset has an approximate resolution of 127 pixels per inch (PPI) in width and 125 PPI in height.

Circular Knitting Machine. The TSfabrics collection comprises fabrics produced on a double-jersey circular knitting machine with a 52-inch cylinder diameter. The machine supports needle gauges from 20G to 30G, enabling the production of fabrics with varying loop densities and surface textures. Depending on the fabric type

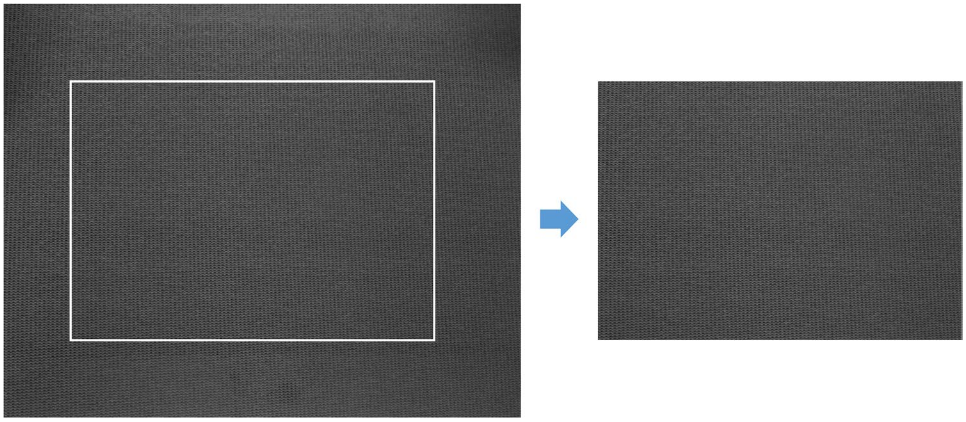

Fig. 6 The original 1280 × 1024 fabric image (left) and the 800 × 640 center-cropped region (right) used to remove corner shadowing and standardize inputs for evaluation.

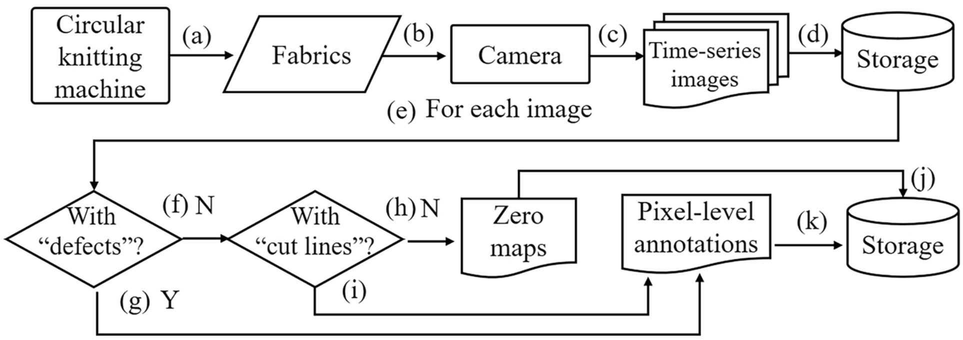

Fig. 7 Pipeline of time-series fabric image collection and annotation.

and yarn properties, the machine operates at rotational speeds of 5-40 RPM, where "RPM" denotes the rotational speed of the circular knitting machine during image acquisition.

Pipeline of Data Collection. Figure 7 provides an overview of the pipeline for the time-series fabric image collection and annotation. First, in Fig. 7(a), circular knitting machines (i.e., Fig. 3(a)) produce various types of fabrics with different textures during the production process. Next, in Fig. 7(b)-(c), we use a camera (i.e., Fig. 3(b)) operating at a fixed capture rate under different illumination conditions to capture time-series fabric images. Furthermore, in Fig. 7(d), these time-series fabric images are stored in a computer (i.e., Fig. 3(c)) for subsequent processing. Moreover, in Fig. 7(e), we apply different annotation methods tailored to each type of fabric image. In particular, we first determine whether each fabric image contains any defects. In Fig. 7(g), we use non-zero values to annotate the corresponding defective regions in the ground truth segmentation maps for fabric images containing defects. For defect-free fabric images in Fig. 7(f), we determine whether each image contains cutlines. For defect-free fabric images without marked cutlines in Fig. 7(h), we use zero maps of the same size as the fabric images as the ground truth segmentation maps. For defect-free fabric images with marked cutlines in Fig. 7(i), we annotate the cutlines using non-zero values in the ground truth segmentation maps. Note that in actual production, "cutlines" are intentionally marked to facilitate subsequent segmentation and processing. Therefore, these defect-free fabric images with marked cutlines are categorized as normal samples. In real-world scenarios, fabric defect detection models also face the challenge of distinguishing between true defects and these intentional cutlines. Here, we provide examples of defect-free fabric images without marked "cutlines" in Fig. 4, defect-free fabric images with marked "cutlines" Fig. 8, and fabric images with defects in Fig. 10. Finally, in Fig. 7(j)-(k), we store these paired fabric images along with their corresponding ground-truth segmentation maps.

Data Records

Overview of TSfabrics. The **TSfabrics** dataset is accessible at Figshare[17]. **TSfabrics** encompasses 22 real and continuous fabric production scenarios featuring different fabric types, production speeds, and lighting environments. Roughly, **TSfabrics** consists of 89900 normal fabric images and 3296 abnormal fabric images. Abnormal fabric images account for 3.54% of the total fabric images. Each fabric image is an 800*640 resolution grayscale image in JPEG format (.jpeg). Figure 9 illustrates the folder structure of the proposed **TSfabrics** dataset. In particular, **TSfabrics** consists of two main folders: IMAGE and ANNOTATION, each containing 22 subfolders

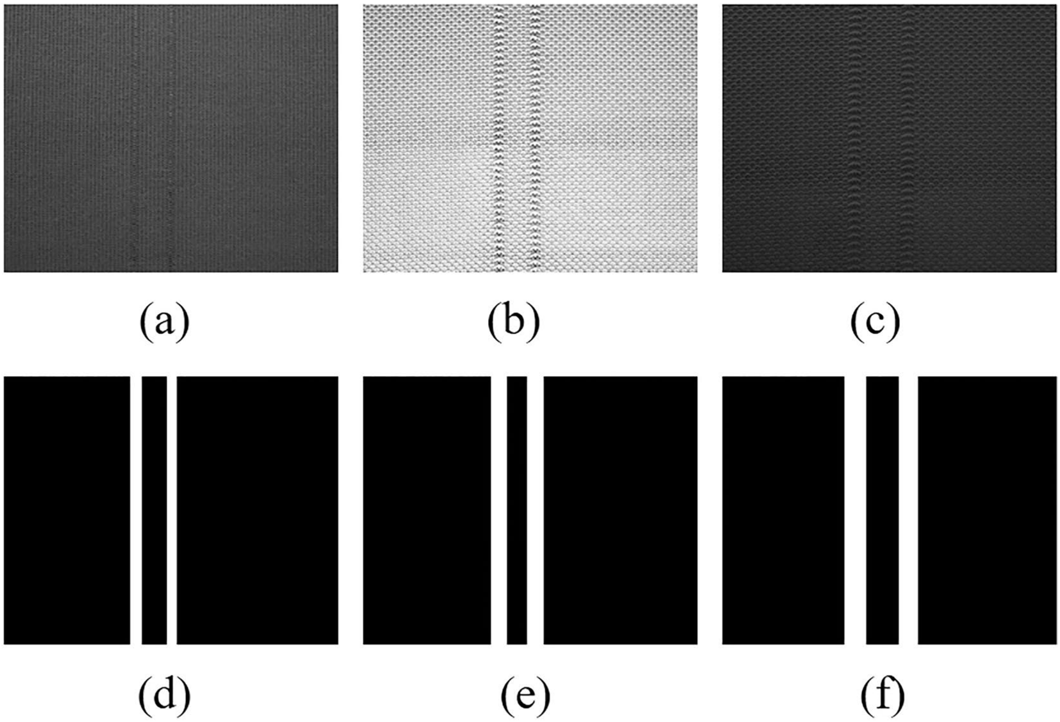

Fig. 8 Examples of defect-free fabric images with marked "cutlines", i.e., (**a**)-(**c**), and their corresponding ground truth segmentation maps, i.e., (**d**)-(**f**).

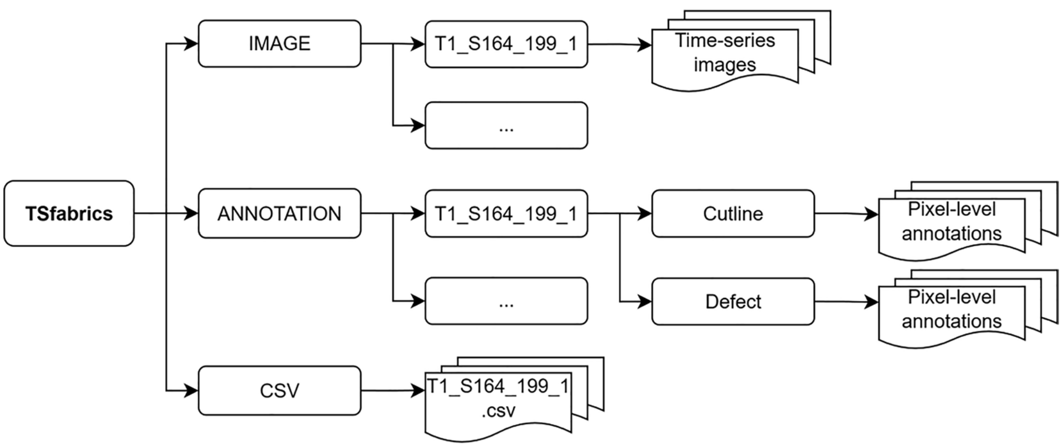

Fig. 9 The folder structure of the proposed **TSfabrics** dataset.

(i.e., the folders listed in Table 2). The subfolders under IMAGE contain the corresponding time-series fabric images. In addition, ANNOTATION contains two folders: Cutline and Defect In addition, each subfolder under ANNOTATION contains two folders—Cutline and Defect—which store the corresponding pixel-level annotations of the time-series fabric images.

Table 1 provides an overview of the proposed **time-series** dataset. First, "Folders" represent sets of fabric images with a specific texture, captured under particular lighting conditions, production speeds, and fabric materials. "Texture" indicates the type of fabric texture. Next, "Speed" indicates the production speed, which affects the number of fabric images collected within a fixed time. Furthermore, "Lighting" indicates the illumination condition. Moreover, "Normal," "Defect," and "Total" represent the number of defect-free fabric images, abnormal fabric images, and the total number of images, respectively. In particular, the names of the "Folders" follow the format {}_{}_{}_{}, where the first placeholder indicates the fabric **T**exture types, including texture 1: Double Piqué (Plain Knit), texture 2: Double Piqué (Four-Corner PK), and texture 3: Double Piqué (Six-Corner PK), the second represents the production **S**peed (with the value of frames per rotation), the third denotes the **I**llumination (with the value of gray values), and the fourth specifies the index of collected fabric images under the same texture, production speed, and lighting condition. Finally, "w/o cutlines" and "w cutlines" represent the

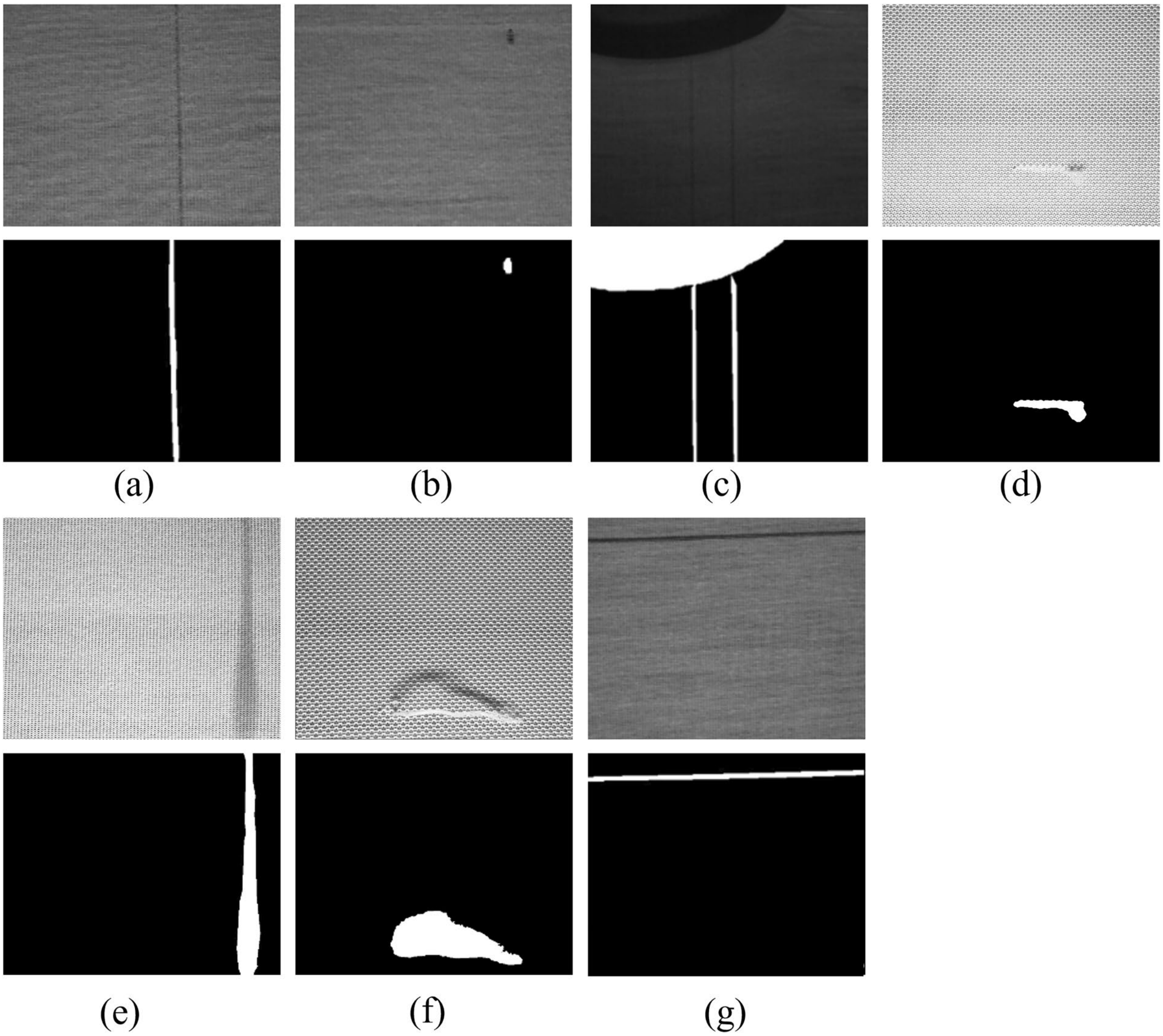

Fig. 10 Examples of fabric images with defects, including (**a**) dropped stitch, (**b**) hole, (**c**) missed stitch, (**d**) fiber lint, (**e**) oil stain, (**f**) distortion, and (**g**) color deviation and their corresponding ground truth segmentation maps.

number of defect-free fabric images without and with cutlines, respectively, in the dataset. In addition, the seven defect descriptions under "Defect" are detailed in the subsequent section "Normal Fabric Types and Diverse Fabric Defect Types."

Characteristics of TSfabrics. In this section, we introduce the key characteristics of the proposed **TSfabrics**, including its time-series nature, fabric types, production periods and "cutlines," production speeds, lighting conditions, and the diversity of fabric defect types.

Time-Series Characteristic. **TSfabrics** consists of continuous and time-series fabric images that accurately reflect real-world continuous knitting production scenarios. Figure 2 provides examples of defect-free time-series fabric images. These time-series fabric images enable fabric defect detection models to learn and leverage the inherent consistency and regularity of normal fabric patterns across adjacent frames, thereby facilitating the more effective identification of subtle or transient defects.

Fabric Types. **TSfabrics** includes three types of well-known fabric textures: Double Piqué (Plain Knit), Double Piqué (Four-Corner PK), and Double Piqué (Six-Corner PK). In Fig. 5, we present representative examples of these three fabric types to illustrate their structural and visual differences under different illumination conditions. Specifically, Fig. 5(a),(c),(e),(g),(i),(k), are captured under well-lit conditions, while Fig. 5(b),(d),(f),(h),(j),(l) are captured under relatively low-illumination conditions. Figure 5(a),(b),(g),(h) correspond to Double Piqué (Plain Knit); Fig. 5(c),(d),(i),(j) correspond to Double Piqué (Four-Corner PK); and Fig. 5(e),(f),(k),(l) correspond to Double Piqué (Six-Corner PK). In addition, Table 2 provides additional detailed information on three fabric types included in the proposed **time-series** dataset. First, "Folders" record a set of fabric images with a specific

Folder	Texture	Speed	Illumination	Normal		Defect							Total
				w/o_cutline	w_cutline	V Line	Hole	Cutline with defect	Fiber lint	Oil stain	Impression mark	H Line	
T1_S164_I199_1		164	199	1161	51	0	0	0	0	0	0	0	1212
T1_S164_I192_1		164	192	967	43	0	0	0	0	10	0	0	1020
T1_S164_I193_1		164	193	987	40	0	0	0	0	0	10	0	1037
T1_S164_I36_1		164	36	1733	74	0	0	0	0	0	0	0	1807
T1_S179_I35_1		179	35	1732	75	0	0	0	0	0	0	0	1807
T1_S174_I108_1		174	108	390	74	60	65	0	0	0	0	28	617
T1_S177_I108_1	Double Piqué (Plain Knit)	177	108	15749	682	0	0	0	0	0	0	0	16431
T1_S174_I111_1		174	111	17838	786	0	0	0	6	0	0	0	18630
T1_S148_I108_1		148	108	2370	145	0	706	41	0	0	0	0	3262
T1_S148_I108_2		148	108	4428	209	167	0	0	0	0	0	0	4804
T1_S555_I117_1		555	117	15938	765	0	1762	0	0	0	0	0	18465
T1_S478_I118_1		478	118	2895	104	0	245	3	0	0	0	0	3247
T1_S478_I118_2		478	118	2961	126	117	0	0	0	0	0	0	3204
T2_S466_I39_1		466	39	4099	191	0	0	0	0	0	0	0	4290
T2_S287_I185_1		287	185	1051	51	0	0	0	61	15	0	0	1178
T2_S287_I184_1	Double Piqué (Four-Corner PK)	200	184	1729	78	0	0	0	0	0	0	0	1807
T2_S262_I52_1		262	52	1549	73	0	0	0	0	0	0	0	1622
T2_S262_I45_1		262	45	1461	65	0	0	0	0	0	0	0	1526
T2_S303_I44_1		303	44	1725	83	0	0	0	0	0	0	0	1808
T3_S165_I175_1		165	175	1731	76	0	0	0	0	0	0	0	1807
T3_S165_I178_1	Double Piqué (Six-Corner PK)	165	178	1727	81	0	0	0	0	0	0	0	1808
T3_S165_I178_2		165	178	1733	74	0	0	0	0	0	0	0	1807
Total	—	—	—	85954	3946	344	2778	44	67	25	10	28	93196

Table 1. Overview of the proposed **time-series** fabric dataset (**TSfabrics**).

texture, captured under particular lighting conditions, production speeds and fabric material. Next, "Texture" indicates the type of fabric texture. "RPM" denotes the rotational speed of the circular knitting machine during image acquisition. Furthermore, "Material" refers to the yarn types used, including 200D/1 and 150D/1 denier filament yarns, as well as 30S/1 cotton yarn. Moreover, "Gauge" denotes the needle density of the knitting machine, including 20G, 24G, or 28G, which determines the fineness of the knitted structure. Finally, "Color" specifies the visual appearance of the greige fabrics, categorized as either white or off-white. As observed from Table 2, the three fabric types differ not only in texture but also in knitting density, denoted as Gauge, with 28G for Double Piqué (Plain Knit), 24G for Double Piqué (Four-Corner PK), and 20G for Double Piqué (Six-Corner PK). In addition, Plain Knit is produced using either a single yarn material (150D/1) or a combination of different materials (200D/1 and 30S/1), whereas Four-Corner PK and Six-Corner PK are produced using a single yarn material only (150D/1). Plain Knit also includes two colors, White and Off-white, whereas Four-Corner PK and Six-Corner PK are available in White only.

Production Period and cutlines. In real-world fabric manufacturing, circular knitting machines mark the fabric with a cutline after completing the full production period, as shown in Fig. 1. Figure 8 presents examples of defect-free fabric images that feature marked cutlines produced during manufacturing. As these marked cutlines are intended to facilitate subsequent manufacturing processes and cutting operations, they should not be regarded as fabric defects. Thus, we categorize fabric images marked with cutlines as normal samples in our dataset.

Production Speed. As different types of fabric textures exhibit varying levels of complexity, circular knitting machines operate at different production speeds during the manufacturing process to accommodate the specific characteristics of each fabric type. Figure 2 shows examples of defect-free time-series fabric images at different production speeds. The circular knitting machines produce different fabrics at speeds ranging from 5 to 30 revolutions per minute (RPM), as shown in Table 2. Since the camera captures fabric images at a constant rate of 30 frames per second, the machine speed directly determines the number of frames captured per production cycle (i.e., one full rotation). Higher speeds (closer to 30 RPM) result in fewer frames per rotation due to the increased rotational velocity, whereas lower speeds (around 5 RPM) yield significantly more frames within the same cycle. In Table 1, a high production speed indicates that the number of fabric images captured within a single production period (i.e., frames per rotation) ranges from 100 to 20 Regular speed corresponds to 200 to 300 images per period, whereas low speed refers to more than 300 images captured in a single production period. A higher production speed implies that fewer fabric images are captured within the same production period.

Folder	Texture	RPM	Materia			Gauge			Color	
			200D/1	150D/1	30S/1	28	24	20	white	off white
T1_S164_I199_1	Double Piqué (Plain Knit)	18		✓		✓			✓	
T1_S164_I192_1		18		✓		✓			✓	
T1_S164_I193_1		18		✓		✓			✓	
T1_S164_I36_1		18	✓		✓	✓				✓
T1_S179_I35_1		18	✓		✓	✓				✓
T1_S174_I108_1		18	✓		✓	✓				✓
T1_S177_I108_1		18	✓		✓	✓				✓
T1_S174_I111_1		18	✓		✓	✓				✓
T1_S148_I108_1		28	✓		✓	✓				✓
T1_S148_I108_2		28	✓		✓	✓				✓
T1_S555_I117_1		28		✓		✓			✓	
T1_S478_I118_1		8		✓		✓			✓	
T1_S478_I118_2		8		✓		✓			✓	
T2_S466_I39_1	Double Piqué (Four-Corner PK)	10		✓				✓	✓	
T2_S287_I185_1		15		✓				✓	✓	
T2_S200_I184_1		25		✓				✓	✓	
T2_S262_I52_1		38		✓				✓	✓	
T2_S262_I45_1		38		✓				✓	✓	
T2_S303_I44_1		20		✓				✓	✓	
T3_S165_I175_1	Double Piqué (Six-Corner PK)	30		✓			✓		✓	
T3_S165_I178_1		30		✓			✓		✓	
T3_S165_I178_2		30		✓			✓		✓	

Table 2. The Detailed information of three fabric types.

Illumination Conditions. Illumination conditions naturally vary over time in real-world fabric manufacturing processes. Meanwhile, to reduce deployment costs when scaling anomaly detection models on production lines, the cameras used for image capture are not equipped with photosensitive components. Consequently, the captured grayscale images were significantly affected by the lighting conditions. Figure 4 shows examples of collected fabric images under varying lighting conditions during production, including dark, normal, and bright illuminations. In particular, the grayscale values of fabric images are typically below 70 under dark illumination conditions, range between 70 and 140 under normal illumination, and exceed 140 under bright illumination conditions.

Normal Fabric Types and Diverse Fabric Defect Types. We provide a CSV file in each folder that records the category of each image. First, **TSfabrics** encompasses two types of normal fabrics:

- **Normal Fabrics without Cutline**: A defect-free fabric image has no cutline impressions, as shown in Fig. 5, and its corresponding label recorded in the CSV file within the respective folder is 1.
- **Normal Fabrics with Cutline**: A defect-free fabric image has cutline impressions, as shown in Fig. 8, and its corresponding label recorded in the CSV file within the respective folder is 2.

TSfabrics encompasses a diverse range of fabric defect types. These defects naturally arise from the machine during production. Figure 10 presents fabric images exhibiting seven types of defects:

- Dropped Stitch (V line): Occurs when certain needles fail to form loops, leading to localized loop loss and vertical indentations. The yarn is still present but fails to form a complete stitch structure, as shown in Fig. 10(a). The corresponding label recorded in the CSV file within the respective folder is 3.
- **Hole**: A visible perforation in the fabric caused by broken needles, leading to a complete loss of yarn structure and compromising the integrity of the fabric surface, as shown in Fig. 10(b). The corresponding label recorded in the CSV file within the respective folder is 4.
- **Missed Stitch (Cutline with Defect)**: During the yarn feeding process, some needles do not engage properly, or the yarn slips past the needles, resulting in interrupted or sparse yarn regions—typically larger in area than dropped stitches, as shown in Fig. 10(c). The corresponding label recorded in the CSV file within the respective folder is 5.
- **Fiber Lint**: Accumulated loose fibers or lint on the fabric surface create small, irregular bright or dark spots that disrupt the local texture, as shown in Fig. 10(d). The corresponding label recorded in the CSV file within the respective folder is 6.
- **Oil Stain**: Greasy stains appear on the fabric surface, typically originating from machine lubricants, operator handling, or environmental contamination, often visible as dark patches or streaks, as shown in Fig. 10(e). The corresponding label recorded in the CSV file within the respective folder is 7.
  Oil stains appear as localized intensity depressions or elongated dark streaks across the fabric surface.

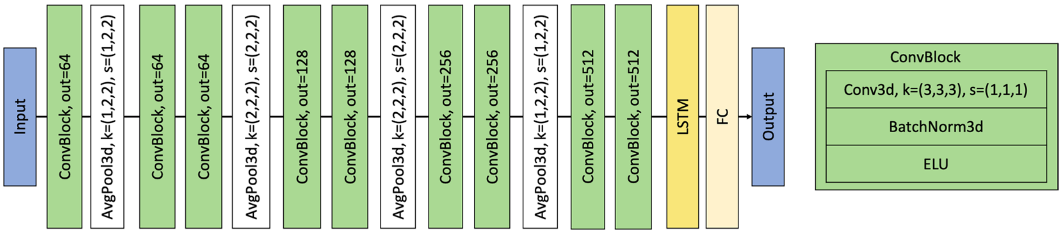

Fig. 11 Network architecture of TSFDNet.

- **Distortion (Impression mark)**: The fabric structure becomes deformed due to tension imbalance, pulling, or compression during production, causing twisting or local thickness anomalies that disrupt surface flatness and appearance, as shown in Fig. 10(f). The corresponding label recorded in the CSV file within the respective folder is 8.
- **Color Deviation (H line)**: A region of the fabric displays a color that differs noticeably from the rest, typically due to uneven dyeing, yarn batch inconsistencies, or irregular oil application, resulting in a visually apparent color mismatch, as shown in Fig. 10(g). The corresponding label recorded in the CSV file within the respective folder is 9.

Technical Validation

In this section, we validate the usability of the proposed dataset. Given that it involves relatively complex real-world production settings, we further provide two illustrative examples to demonstrate how it can be employed for potential experiments and evaluations. We first introduce the implementation details and evaluation metrics to help readers easily follow the evaluation process. Next, we report the performance results to investigate the potential challenges faced when deploying fabric defect detection models in actual production environments.

Implementation detail. First, we use 3D ResNet-18[19] as the backbone and follow the model construction in[20] by additionally incorporating a single-layer LSTM[21] and a fully connected layer to construct the baseline model (Time-Series Fabric Detection Net, TSFDNet), as shown in Fig. 11. During both training and testing stages, the models are fed non-overlapping sequences of 12 consecutive fabric images at a time. Next, we follow[22] to use the cross-entropy to constrain the baseline model for image classification.

Evaluation metrics. To ensure a fair comparison with previous methods, we adopt evaluation metrics that are widely used in the field of fabric defect detection, including **Precision, Recall**, and **F1-score**[23]. These metrics provide a comprehensive assessment of a model's detection accuracy and robustness:

- **Precision** measures the proportion of correctly identified defective fabric images among all images predicted as defective. Higher precision indicates fewer false positives, which is crucial in industrial settings to avoid unnecessary halts in production.

$$Precision = \frac{TP}{TP + FP} \tag{1}$$

where TP is the number of true positive defect detections, and FP is the number of false positives.
- **Recall** (also known as sensitivity) assesses the model's ability to detect actual defects. A high recall is essential to ensure that real defects are not overlooked during inspection.

$$Recall = \frac{TP}{TP + FN} \tag{2}$$

where FN is the number of false negatives, i.e., defects that the model failed to detect.
- **F1-score** is the harmonic mean of Precision and Recall, offering a balanced measure that considers both correctness and completeness of defect detection:

$$F1 = 2 \times \frac{Percision \times Recall}{Percision + Recall} \tag{3}$$

These metrics collectively evaluate the accuracy and robustness of fabric defect detection models, especially under complex and variable conditions present in real-world manufacturing environments.

Example Evaluations. In Tables 3 and 4, we provide two illustrative examples to guide readers on how the proposed dataset can be employed for potential experiments and evaluations. In particular, we validate the usability of the dataset by examining the effects of illumination variation and production speed, respectively. We train

Train Data	Test Data	Similar Speed?	Similar Illumination?	Precision	Recall	F1
T1_S164_I192_1 (high speed, bright illumination)	T1_S164_I199_1	✓(high)	✓(bright)	83.28%	66.58%	74.00%
	T1_S164_I193_1	✓(high)	✓(bright)	92.87%	86.53%	89.59%
	T1_S164_I36_1	✓(high)	× (dark)	67.95%	50.00%	57.61%
	T1_S179_I35_1	✓(high)	× (dark)	67.92%	50.00%	57.60%
	T1_S174_I108_1	✓(high)	× (regular)	21.08%	33.33%	25.83%
	T1_S177_I108_1	✓(high)	× (regular)	47.93%	50.00%	48.94%
	T1_S174_I111_1	✓(high)	× (regular)	31.92%	33.33%	32.61%
	T1_S148_I108_1	✓(high)	× (regular)	57.56%	33.42%	42.29%
	T1_S148_I108_2	✓(high)	× (regular)	30.75%	33.33%	31.99%
T2_S287_I185_1 (middle speed, bright illumination)	T2_S466_I39_1	× (low)	× (dark)	49.94%	49.78%	49.86%
	T2_S287_I184_1	✓(middle)	✓(bright)	81.74%	82.26%	82.00%
	T2_S262_I52_1	✓(middle)	× (dark)	59.73%	59.00%	59.36%
	T2_S262_I45_1	✓(middle)	× (dark)	60.41%	61.61%	61.00%
	T2_S303_I44_1	× (low)	× (dark)	59.72%	53.29%	56.32%
T3_S165_I175_1 (high speed, bright illumination)	T3_S165_I178_1	✓(high)	✓(bright)	97.81%	91.23%	94.41%
	T3_S165_I178_2	✓(high)	✓(bright)	97.98%	90.68%	94.18%

Table 3. Evaluation results under varying illumination with similar production speeds.

Train Data	Test Data	Similar Speed?	Similar Illumination?	Precision	Recall	F1
T1_S245_I119_1 (middle speed, regular illumination)	T1_S174_I108_1	× (low)	✓(regular)	37.66%	42.75%	40.05%
	T1_S177_I108_1	× (low)	✓(regular)	33.29%	31.64%	32.44%
	T1_S174_I111_1	× (low)	✓(regular)	33.35%	42.42%	37.34%
	T1_S148_I108_1	× (low)	✓(regular)	40.05%	40.86%	40.45%
	T1_S148_I108_2	× (low)	✓(regular)	39.96%	58.90%	47.62%
	T1_S555_I117_1	× (high)	✓(regular)	86.35%	91.85%	89.01%
	T1_S478_I118_1	× (high)	✓(regular)	92.81%	87.82%	90.25%

Table 4. Evaluation results under similar illumination with varying production speeds.

fabric defect detection models using time-series fabric images and their corresponding ground truth labels with cross-entropy loss to evaluate the effectiveness of the proposed TSfabrics dataset.

Evaluation under Varying Illumination with Similar Production Speeds. In Table 3, we present an example that investigates the impact of similar production speeds but varying illumination conditions on the performance for fabric defect detection models.

First, in Table 3, we compare the performance under **similar production speeds and lighting conditions** between the source training data and the target testing data, specifically in the cases of T1_S164_I199_1, T1_S164_I193_1, T2_S287_I184_1, T3_S165_I178_1, and T3_S165_I178_2. We observe that fabric defect detection models demonstrate promising performance (i.e., average precision 90.74%, average recall 83.46%, and average f1-score 86.84%) in these cases when evaluating fabric images collected under comparable production speeds and lighting conditions to the training environment.

Next, we compare performance under **similar production speeds and varying lighting conditions** between the source training data and the target testing data, specifically in the cases of T1_S164_I36_1, T1_S179_I35_1, T1_S174_I108_1, T1_S177_I108_1, T1_S174_I111_1, T1_S148_I108_1, T1_S148_I108_2, T2_S262_I52_1, and T2_S262_I45_1. We observe that detection performance significantly degrades (i.e., average precision 53.02%, average recall 46.34%, and average f1-score 48.93%) under illumination variations, especially as the lighting conditions in the target domain become more severe. Therefore, illumination variation poses a critical challenge that must be addressed for effective real-world fabric defect detection.

Evaluation under Similar Illumination with Varying Production Speeds. In Table 4, we present an example that investigates the impact of similar illumination conditions but varying production speeds on the performance of fabric defect detection models.

First, we compare performance under **low production speeds under similar lighting conditions** between the source training data and the target testing data, specifically in the cases of T1_S174_I108_1, T1_S177_I108_1, T1_S174_I111_1, T1_S148_I108_1, and T1_S148_I108_2. In these cases of low production speeds, we observe that fabric defect detection models tend to perform poorly (i.e., average precision 36.86%, average recall 43.31%, and average f1-score 39.58%) when detecting fabric images collected at lower production speeds than those used in the source training data.

Next, we compare performance under **high production speeds under similar lighting conditions** between the source training data and the target testing data, specifically in the cases of T1_S555_I117_1 and T1_S478_I118_1. We observe that fabric defect detection models can still achieve promising performance (i.e., average precision 89.58%, average recall 89.83%, and average f1-score 89.63%) in these cases when detecting fabric images collected at higher speeds than those seen in the source training data. By comparing the cases of low and high production speeds in Table 4, we observe that fabric defect detection models are generally more robust to higher production speeds (i.e., average precision 89.58%, average recall 89.83%, and average f1-score 89.63%) but struggle to maintain performance when faced with lower production speeds than those seen during training (i.e., average precision 36.86%, average recall 43.31%, and average f1-score 39.58%).

Usage Notes

The **TSfabrics** dataset will be publicly released under the Creative Commons Attribution 4.0 International License (CC BY 4.0). **TSfabrics** will be openly accessible for academic and research purposes. Researchers are permitted to download, use, distribute, and modify the dataset. Accordingly, we request that researchers who use this dataset cite this work in their publications.

Data availability

The TSFabrics dataset are publicly accessible via Figshare [24]).

Code availability

The entire code to produce the results of this paper is accessible at: https://github.com/yoyoullllll5/TSFabric.git. We utilized Python and PyTorch in this study.

Received: 22 July 2025; Accepted: 27 January 2026;
Published online: 07 February 2026

References

1. Zhao, P. *et al*. An open paradigm dataset for intelligent monitoring of underground drilling operations in coal mines. *Sci. Data* **12**, 1–16 (2025).
2. Piecuch, G. & Zabiński, T. A new open dataset from a milling process - data for classification and estimation of tool life. *Sci. Data* **12**, 650 (2025).
3. Luh, M. & Blank, T. Comprehensive battery aging dataset: capacity and impedance fade measurements of a lithium-ion nmc/c-sio cell. *Sci. Data* **11**, 1004 (2024).
4. Chen, F.-X. R. *et al*. Deep learning based atomic defect detection framework for two-dimensional materials. *Sci. Data* **10**, 91 (2023).
5. Yu, Z., Xu, Y., Wang, Y., Sheng, X. & Xie, G. Dual-path segmentation network for automatic fabric defect detection. *Textile Res. J.* https://doi.org/10.1177/00405175231192057 (2023).
6. Zhang, T. & Ma, H. Clothnet: sensitive semantic segmentation network for fabric defect detection. *Textile Res. J.* **93**, 103–115 (2023).
7. Song, W., Lang, D., Zhang, J., Zheng, M. & Li, X. Textile defect detection algorithm based on the improved yolov8. *IEEE Access* (2025).
8. Chen, Q., Luo, H., Lv, C. & Zhang, Z. A unified anomaly synthesis strategy with gradient ascent for industrial anomaly detection and localization. In *European Conference on Computer Vision*, 37–54 (Springer, 2024).
9. Liu, X., Wang, J., Leng, B. & Zhang, S. Unlocking the potential of reverse distillation for anomaly detection. In *Proceedings of the AAAI Conference on Artificial Intelligence*, vol. 39, 5640–5648 (2025).
10. Sträter, L. P., Salehi, M., Gavves, E., Snoek, C. G. & Asano, Y. M. Generalad: Anomaly detection across domains by attending to distorted features. In *European Conference on Computer Vision*, 448–465 (Springer, 2024).
11. Huang, P.-K. *et al*. One-class face anti-spoofing via spoof cue map-guided feature learning. In *IEEE/CVF Conference on A Two-Branch Multidirectional*, 277–286 (2024).
12. Huang, P.-K. *et al*. Slip: Spoof-aware one-class face anti-spoofing with language image pretraining. In *Proceedings of the AAAI Conference on Artificial Intelligence*, vol. 39, 3697–3706 (2025).
13. Ma, C., Qi, L., Wang, Y., Wang, W. & Sun, Y. Improving lightweight model for fabric defect segmentation via contrastive knowledge distillation. In *Third International Conference on Advanced Algorithms and Neural Networks (AANN 2023)*, vol. 12791, 404–409 (SPIE, 2023).
14. Shi, Y., Yang, J. & Qi, Z. DFR: Deep feature reconstruction for unsupervised anomaly segmentation. *Neurocomputing* **424**, 9–22 (2021).
15. Xi, Y., Zhang, Y., Ding, S. & Wan, S. Visual question answering model based on visual relationship detection. *Signal Process. Image Commun.* **80**, 115648 (2020).
16. Zhang, C., Feng, S., Wang, X. & Wang, Y. ZJU-Leaper: A benchmark dataset for fabric defect detection and a comparative study. *IEEE Transactions on Artif. Intell.* **1**, 219–232 (2020).
17. Ni, Y.-Q., Huang, P.-K., Wang, W.-J. & Liang, D. Tsfabrics: A time-series fabric dataset for real-time defect detection on circular knitting machines. *Sci. data*. https://doi.org/10.6084/m9.figshare.29573381 (2026).
18. Zhang, H.-W., Zhang, L.-J., Li, P.-F. & Gu, D. Yarn-dyed fabric defect detection with yolov2 based on deep convolution neural networks. In *2018 IEEE 7th Data Driven Control and Learning Systems Conference (DDCLS)*, 170–174 (IEEE, 2018).
19. He, K., Zhang, X., Ren, S. & Sun, J. Deep residual learning for image recognition. In *Proceedings of the IEEE Conference on Computer Vision and Pattern Recognition*, 770–778 (2016).
20. You, J. & Korhonen, J. Deep neural networks for no-reference video quality assessment. In *2019 IEEE International Conference on Image Processing (ICIP)*, 2349–2353 (IEEE, 2019).
21. Yu, Y., Si, X., Hu, C. & Zhang, J. A review of recurrent neural networks: LSTM cells and network architectures. *Neural Computation* **31**, 1235–1270 (2019).
22. Song, T., Wang, Y., Gao, C., Chen, H. & Li, J. MSLAN: A two-branch multidirectional spectral-spatial LSTM attention network for hyperspectral image classification. *IEEE Trans. Geosci. Remote Sens.* **60**, 1–14 (2022).
23. Khan, A., Chefranov, A. & Demirel, H. Image-level structure recognition using image features, templates, and ensemble of classifiers. *Symmetry* **12**, 1072 (2020).
24. Ni, Y.-Q., Huang, P.-K., Lin, C.-Y., Wang, W.-J. & Liang, D. Tsfabrics: A time-series fabric dataset for real-time defect detection on circular knitting machines. *figshare* https://doi.org/10.6084/m9.figshare.29573381 (2026).

Acknowledgements
This work is jointly developed by the Department of Computer Science and Information Engineering and the Department of Biomedical Engineering of the National Central University. This work is sponsored by the National Science and Technology Council (NSTC) under the project NSTC 113-2222-E-008-002.

Author contributions
Yan-Qin Ni: Data collection, Writing - original draft, Writing - review & editing, Validation, Visualization; **Pei-Kai Huang**: Writing - original draft, Writing - review & editing,Visualization; **Wei-Jen Wang**: Supervision, Project administration; **Deron Liang**: Supervision, Project administration, Funding acquisition; **Chia-Yu Lin** : Supervision, Writing - review & editing, Project administration, Funding acquisition.

Competing interests
The authors declare no competing interests.

Additional information
Correspondence and requests for materials should be addressed to C.-Y.L.

Reprints and permissions information is available at www.nature.com/reprints.

Publisher's note Springer Nature remains neutral with regard to jurisdictional claims in published maps and institutional affiliations.